Effects of oxidation on mechanical and physical properties of ultra-high-modulus and ultra-high-molecular-weight polyethylene fibres

You-Lo Hsieh*, Geoff Barrall and Shanqing Xu†
Division of Textiles, University of California–Davis, Davis, CA 95616, USA
(Received 10 September 1990; revised 26 November 1990; accepted 7 December 1990)

The effects of oxidation on gel-spun ultra-high-modulus and ultra-high-molecular-weight polyethylene (UHMWPE) fibres were investigated. The single-fibre tensile properties of the UHMWPE fibres were lowered by all chromic acid/potassium dichromate oxidation reactions studied. The tensile properties were highly reaction-time-dependent for the fibres treated in the acid-assisted reactions with CrO_3 (**I**) and with $K_2Cr_2O_7$ (**IIa**) at a higher H_2SO_4 concentration (or a 1:20 $K_2Cr_2O_7$:H_2SO_4 weight ratio). The tensile properties of fibres treated in the acid-assisted reaction with $K_2Cr_2O_7$ (**IIb**) at a lower H_2SO_4 concentration (or a 1:1.3 $K_2Cr_2O_7$:H_2SO_4 weight ratio) and the base-catalysed reaction (**III**) were slightly lowered, but were independent of reaction time. The fractured fibre ends from reactions **IIb** and **III** remained fibrillated as observed on the untreated fibres, whereas brittle fractures were observed on those oxidized by reactions **I** and **IIa**. Experimental results indicated that the oxidative agents in reactions **I** and **IIa** penetrated more thoroughly into the fibrillar structures of the fibres than in the base-catalysed reaction **III** and reaction **IIb**. The changes in the tensile and fracture properties suggested different diffusion and oxidative mechanisms between chromic acid (**I**) and potassium dichromate (**IIb**) under similar sulphuric acid-assisted conditions. All oxidative reactions reduced superheating, which resulted in the increased heat of fusion but decreased melting temperatures and narrowed melting peak widths.

(Keywords: ultra-high modulus; ultra-high molecular weight; polyethylene; fibres; oxidative reactions; tensile properties; differential thermal analysis; scanning electron microscopy)

INTRODUCTION

Oxidation of polyethylene has been extensively studied on low-density polyethylene (LDPE). A number of chemical oxidation reactions using either chromic acid or potassium dichromate solutions have been reported[1–6]. These reactions have been shown to induce surface changes such as the addition of functional groups[3–6], improved water wettability[6] and increased adhesion to epoxy resin[3].

Owing to the branched structure of LDPE, oxidative attacks can occur at a variety of sites including tertiary carbons, methylene groups and double bonds. On the linear structure of high-density polyethylene (HDPE), however, oxidative attacks are limited to the methylene groups. Though more limited in the variety of oxidative sites, evidence of possible oxidative reactions on HDPE has been shown by changes in fibre properties. Oxidative treatments similar to those studied on LDPE have been shown to improve the adhesion of high-modulus polyethylene fibres from melt-spinning[7,8] and gel-spinning[7,9] to epoxy resin.

Chemical reactions in polymer solids are diffusion-controlled, and therefore morphological differences in LDPE and HDPE should probably affect chemical accessibility. For ultra-high-modulus and ultra-high-molecular-weight polyethylene (UHMWPE) fibres, the micro- and macrostructures of the fibres are highly dependent upon the extrusion, crystallization and drawing processes[10–13]. For example, gel-spinning[14–16], melt-spinning[17] and solid-state extrusion[18] have been shown to produce fibres with significantly different properties.

The tensile properties of various UHMWPE fibres other than the gel-spun UHMWPE fibres have been reasonably well described by several molecular models[19–21]. Among them, only the model[22,23] that describes a macrofibrillar structure with interconnected molecules explains the tensile behaviour of gel-spun UHMWPE fibres consistently. Gel-spun UHMWPE fibres are believed to consist of macrofibrils of infinite length along the fibre direction. The macrofibrils are about 0.5 μm in diameter and consist of 20 nm diameter microfibrils[24]. The microfibrils are composed of 70 nm long crystal blocks connected by disordered domains about 4 nm long[25]. The disordered domains, which are thought to contain entanglements, chain ends, taut tie molecules (TTM) and other imperfections, are the weakest spots in the microfibrils. Tensile strength in these domains is thought to be transferred by the load-carrying chains such as TTM and entangled chains[26–28]. The elongation at break and the tensile modulus were largely determined by the ratio of disordered-domain length to crystal-block length[29].

* To whom correspondence should be addressed
† Current address: Department of Textile Engineering, Nantong Textile Institute of Technology, Nantong, People's Republic of China

0032-3861/92/030536-10

Unlike LDPE, the understanding of the exact mechanisms and effects of oxidative attacks on HDPE, including UHMWPE fibres, is limited. In this paper, the effects of strain rate on single-fibre tensile properties and the effects of several oxidative reactions on the gel-spun UHMWPE fibres are discussed. Liquid diffusion and chemical reactions in polymers usually occur in the less ordered regions. The studies of oxidative attacks in the gel-spun UHMWPE fibres should therefore provide some insights into the morphology of the fibres.

OXIDATIVE REACTIONS

Several chromic–sulphuric oxidative reactions, including the use of both chromic acid and potassium dichromate, were studied. The reactions included acid-catalysed reactions **I** and **II**, and a base-catalysed reaction **III**. The acid-catalysed reactions involved either chromic acid or potassium dichromate with sulphuric acid, whereas the base-catalysed reaction used potassium dichromate with sodium hydroxide.

Acid-catalysed reactions

I $$CrO_3 + H_2SO_4 \rightarrow CrO_4^{2-} + 2H^+ + SO_3 \quad (1)$$

$$K_2Cr_2O_7 + 2H_2SO_4 \rightarrow 2KHSO_4 + H_2O + 2CrO_3 \quad (2)$$

II $$K_2Cr_2O_7 + 4H_2SO_4 \rightarrow 2KHSO_4 + H_2O + 2CrO_4^{2-} + 4H^+ + 2SO_3 \quad (3)$$

Base-catalysed reaction

III $$Cr_2O_7^{2-} + 2OH^- \rightarrow 2CrO_4^{2-} + H_2O \quad (4)$$

The initial oxidative reactions on linear polyethylene can form hydroxyl side-groups. Further oxidation of the hydroxyl groups can result in ketone–carbonyl groups, then chain cleavage and formation of carboxyl (acid and ester) groups. The mechanisms for these reactions are, however, not well understood.

EXPERIMENTAL

Fibre preparation

The gel-spun UHMWPE fibres studied were Spectra 1000 filaments from Allied Signal Inc. The filaments were wound into looped bundles and tied. These bundles were washed in carbon tetrachloride for 30 min at 23°C and dried in a vacuum desiccator for 2 h. The weights of the cleaned and dried fibres were obtained.

Reagents

All reagents were used without purification. The sulphuric acid was 95–98% in concentration. The potassium dichromate and chromic acid were 99% and 99.9%, respectively.

Oxidation of fibres

The effects of either chromic acid or sulphuric acid alone on UHMWPE fibres were evaluated by 15 min treatments at 23°C. The chromic acid solution had the same 1:1 CrO_3:H_2O weight ratio as in reaction **I**. With sulphuric acid, six concentrations were used. They ranged from a 1:1.45 H_2SO_4:H_2O weight ratio (or 0.007 mol g^{-1}) up to the concentrated acid (or 0.281 mol g^{-1}). Water in sulphuric acid was assumed to be 3.5% and was accounted for in all calculations.

The two acid-catalysed reactions involved H_2SO_4-assisted reactions with either CrO_3 or $K_2Cr_2O_7$. For reaction **I**, a 1:1:1.45 weight ratio of CrO_3:H_2SO_4:H_2O was used. This weight ratio gives the same molar ratio as in equation (1) and is the same as that used by Kato *et al.* on HDPE films[30]. For reactions **II**, two $K_2Cr_2O_7$:H_2SO_4:H_2O weight ratios were evaluated. Reaction **IIa** had a 1:20:1.6 ratio, which was similar to that used by Whiteside *et al.* on LDPE films[4,5]. Reaction **IIb** had a $K_2Cr_2O_7$:H_2SO_4:H_2O ratio of 1:1.33:1.7, which was the same as the 1:4 $K_2Cr_2O_7$:H_2SO_4 molar ratio as in equation (3). The sulphuric acid concentration in **IIa** was 15 times higher than that in **IIb**.

For the acid-catalysed reactions, either chromic acid or potassium dichromate was first dissolved in distilled water while stirring with a glass rod. Sulphuric acid was added slowly to the chromic acid solution. To examine the extent of oxidation attacks, preliminary experiments of reactions **I** and **IIa** were conducted at an elevated temperature of about 68°C for 15 min. The tensile properties of the treated fibres by both treatments were significantly lowered (*Table 1*). It should be noted that the fibres used in these preliminary experiments were from a different batch. The tensile data of the untreated fibres were slightly different from those presented in the rest of this study. The severity of the reactions was reduced by running the reactions at a lower temperature of 23°C. The heat from mixing sulphuric acid with chromic acid was dissipated by using an ice bath. The solution was then allowed to stabilize at 23°C.

The base-catalysed reaction (**III**) involved a 1:0.27:3.3 weight ratio of $K_2Cr_2O_7$:NaOH:H_2O solutions. This weight ratio gives the 1:2 molar ratio of $K_2Cr_2O_7$:NaOH as in equation (4). Potassium dichromate and sodium

Table 1 Tensile properties[a] of sulphuric–chromic treated (at 68°C) Spectra 1000 fibres[b] (gauge length = 25.4 mm and crosshead speed = 20 mm min^{-1})

Sulphuric–chromic reaction	Reaction time (min)	Weight change (%)	Breaking load (g)	Breaking strain (%)
None	0	0	218.0 (34.4)	9.6 (0.9)
CrO_3:H_2SO_4:H_2O 1:1:1.45	15	−11.0	26.8 (20.2)	1.5 (0.8)
K_2Cr_2O:H_2SO_4:H_2O 1:20:1.6	15	+0.3	125.7 (20.2)	5.8 (1.0)

[a]Numbers in parentheses denote standard deviation
[b]Filaments were from a different batch from those for the rest of this study

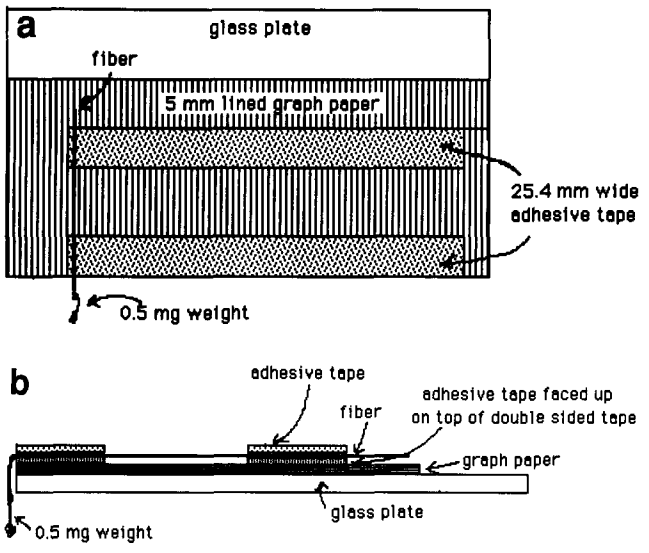

Figure 1 Sample mounting configuration for single-fibre tensile tests: (a) top view, (b) side cross-sectional view

hydroxide were dissolved in water separately. The potassium dichromate solution was heated to 50°C before the sodium hydroxide solution was added and mixed. The mixture was cooled to 23°C before use.

The fibres were treated by submerging fibre bundles in the prepared solutions for reactions **I**, **IIa**, **IIb** and **III** for 1, 5 or 15 min. After the treatments, the fibres were washed with water three times. Surface chromium was removed from the fibres by rinsing in 70% aqueous nitric acid for 3 min. Previous study showed that a harsher nitric acid wash (15 min at 50°C) following similar oxidation reaction on LDPE caused no effect on fibre adhesion property[1]. The fibre bundles were then washed again with three fresh rinses of water before being placed in a vacuum desiccator to be dried. The dry weights of the treated fibres were then obtained.

Tensile properties

An Instron 1122 TM tensile tester equipped with the standard pneumatic and rubber-faced grips was employed for measuring the tensile properties of the single fibres. The variables in tensile testing procedures were examined by varying the gauge lengths and the crosshead speed over a 10-fold and a 500-fold range, respectively. The gauge lengths were varied from 25.4 mm to 254 mm while maintaining a constant crosshead speed of 20 mm min^{-1}. Crosshead speeds ranging from 1 to 500 mm min^{-1} were tested on fibres with a fixed gauge length of 25.4 mm.

A specific fibre mounting procedure was developed to overcome grip slippage and to minimize damage to the UHMWPE fibres. The glass plate assembly for mounting fibres is shown in *Figure 1*. A sheet of graph paper with 5 mm lines was adhered on top of the glass as backing (*Figure 1*). Two rows of 1 inch wide adhesive tapes with their adhesive side up were secured on the backing paper by double-sided tape. The spacing between the two rows of tapes corresponded to the gauge length desired. For the 25.4 mm gauge length, 6 inch long sections of fibres were laid across the adhesive tapes. The fibres were placed 10 mm apart and parallel to each other. The top ends of the fibres were fixed by placing another piece of adhesive tape on top. While maintaining the fibres in the horizontal position, 0.5 mg weights were added to the other ends of all fibres before fixing them with another strip of adhesive tape. This weight was sufficient to minimize the slack between the two taped ends.

Fibre samples were then separated from each other by cutting through the paper backing vertically. The separated individual fibres were supported by 10 mm wide paper backing with a 25.4 mm × 10 mm piece of adhesive tape at each end. The two taped ends of the fibre assembly were then placed in between sample grips on the Instron. The paper backings protected the fibre sections to be tested from any stress or damage during preparation. Immediately before testing, the paper backing was cut apart perpendicular to the fibre axis. All tensile tests were performed at 23°C and 65% relative humidity.

Differential thermal analysis

D.t.a. in nitrogen was performed on the untreated as well as the oxidized polyethylene fibres. For each of the oxidative reactions, the fibres treated longest (15 min) were chosen. About 3.5–4 mg of fibres was packed at the bottom of a sample pan. A Mettler TA 2000M Analyzer was employed for the d.t.a. runs from 30 to 200°C at a heating rate of 5°C min^{-1}. The heat of fusion ($J\,g^{-1}$) was derived from converting the area under the melting peak using indium calibration.

Scanning electron microscopy

The fibres were mounted with silver conductive paint and dried in a vacuum oven for 12 h. The samples were then coated with a 300 Å gold layer by two consecutive sputterings to avoid possible heat damage to the material. An International Scientific Instrument model DS 130 SEM was used for fibre surface evaluation.

RESULTS AND DISCUSSION

Tensile properties of untreated fibres

The strain-rate effects on the tensile properties of the untreated fibres were evaluated by varying either the gauge length at a constant crosshead speed or the crosshead speed at a constant gauge length. By dividing the crosshead speed with the gauge length, the strain rate in reciprocal minutes was obtained. With the described variation, the strain rates increased with increasing crosshead speeds at a constant gauge length. At constant crosshead speed, on the other hand, strain rates decreased with increasing gauge lengths. The values of modulus at 100 g of load were taken for comparison among fibres.

The effects of a broad range of crosshead speeds from 1 to 500 mm min^{-1} were evaluated at a constant gauge length of 25.4 mm. Both breaking load (*Figure 2a*) and modulus (*Figure 2c*) increased initially with the crosshead speeds up to 20 mm min^{-1} (or a 0.787 min^{-1} strain rate). The positive strain-rate effect on tensile strength of Spectra 1000 fibres in the lower strain-rate range up to 1.0 min^{-1} was the same as that reported on Spectra 900 filaments when crosshead speed was varied[31]. The higher crosshead speeds (up to 20 min^{-1}) examined in this study showed additional strain-rate effects on the tensile behaviour of Spectra 1000 fibres. Above the 20 mm min^{-1} crosshead speed, the breaking load and modulus decreased with increasing crosshead speed to levels below those obtained at the lowest crosshead speed. The breaking strain reduced significantly as the crosshead

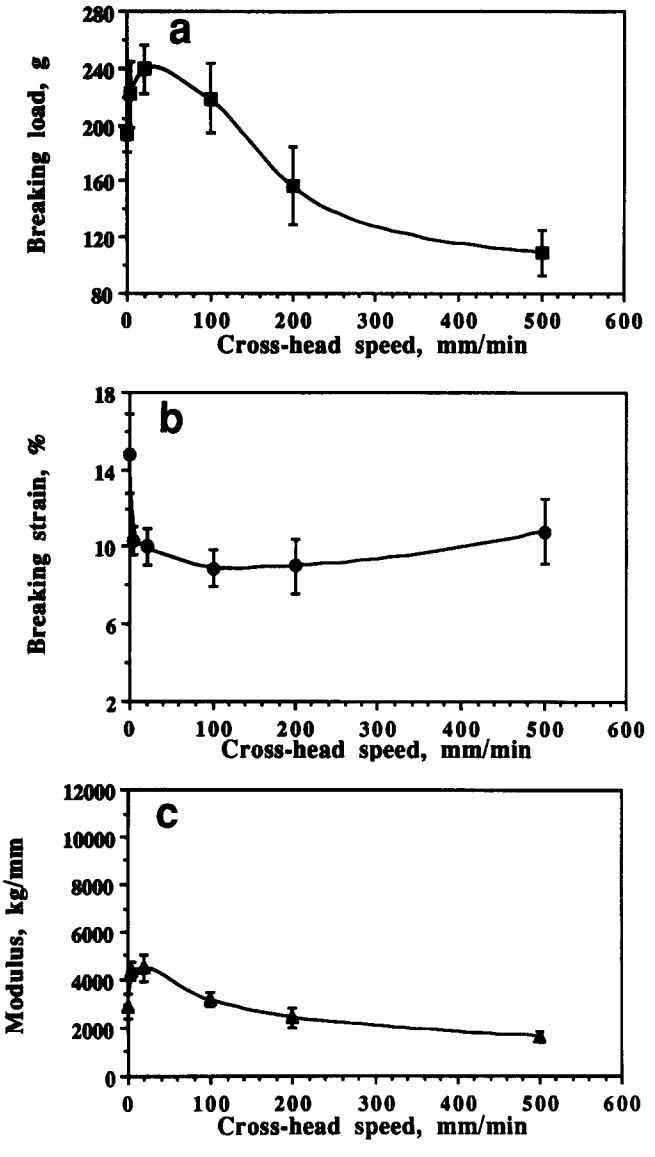

Figure 2 Crosshead speed effects on the single-fibre tensile properties of the untreated fibres at a constant 25.4 mm gauge length: (a) breaking load, (b) breaking strain, (c) modulus at 100 g load

speed increased to 20 mm min^{-1}, but became independent of further gauge length increases (*Figure 2b*).

At a constant crosshead speed of 20 mm min^{-1}, significant reduction in the breaking load (*Figure 3a*) and the breaking strain (*Figure 3b*) as well as significant increase in modulus (*Figure 3c*) were observed with increasing gauge length to 50.8 mm. The load at break remained unchanged with further increases in gauge length. The changes in breaking strain and modulus continued gradually with further increases in gauge length.

These tensile data obtained from varying both gauge lengths and crosshead speeds were combined in *Figure 4*. Significant scattering in tensile properties was observed on the combined strain-rate series, especially at the very low strain rates up to 0.787 min^{-1}. The breaking loads peaked at a strain rate of 0.787 min^{-1} and then decreased with further strain-rate increases (*Figure 4a*). The modulus and breaking strain data varied significantly up to 0.787 min^{-1}, then levelled off with increasing strain rate (*Figures 4b* and *4c*).

The optimal tensile properties were observed at the 20 mm min^{-1} crosshead speed. The highest breaking load (239 g) was obtained with the 25.4 mm gauge length, whereas the highest modulus (9101 kg mm^{-2}) and the lowest breaking strain (4.0%) were found with a much longer 254 mm gauge length. For reasonable sample preparation and testing time, a 25.4 mm gauge length and a crosshead speed of 20 mm min^{-1} with an equivalent strain rate of 0.787 min^{-1} were used for comparisons between the untreated and oxidized fibres. Under this condition, the modulus was found to increase with load and levelled off at loads above 80 g (*Figure 5*). As indicated earlier, all comparisons on modulus were made using data at 100 g load. In the range of strain rate studied, the selected condition gave a maximum breaking load of 239 g but moderate modulus and breaking strain of 4426 kg mm^{-2} and 10.0%, respectively, for the untreated fibres.

Weight change after oxidation

At 68°C, severe weight losses were observed on oxidized fibres (*Table 1*). At a lower reaction temperature of 23°C, however, the weight changes from the various oxidation reactions were less than 1% (*Table 2*). Although weight gains could be explained by residual chromium salts and weight loss could be due to fibre loss, the observed changes were too small to justify their significance in either case.

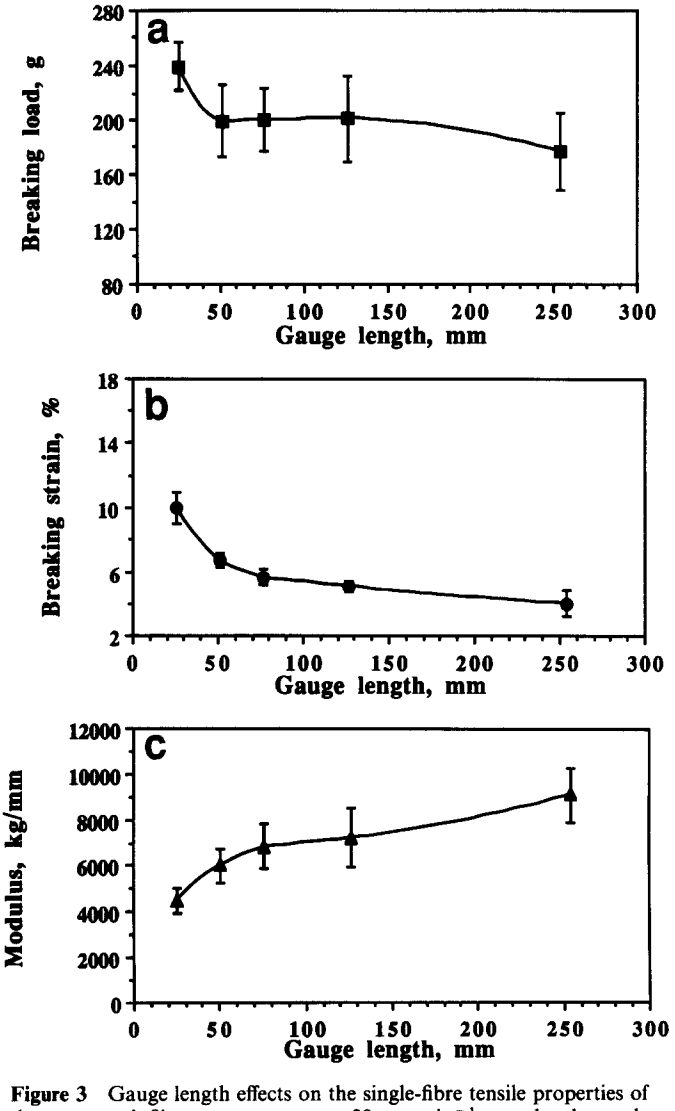

Figure 3 Gauge length effects on the single-fibre tensile properties of the untreated fibres at a constant 20 mm min^{-1} crosshead speed: (a) breaking load, (b) breaking strain, (c) modulus at 100 g load

Tensile properties of oxidized fibres

The tensile properties of the UHMWPE fibres treated in either chromic acid or sulphuric acid alone were evaluated first. The treatment in chromic acid solution with the same CrO_3:H_2O weight ratio as in reaction **I** was not found to affect any of the tensile properties. The treatments in sulphuric acid were performed at a range of concentrations (*Table 3*). The 1:1.45 and 12.5:1 H_2SO_4:H_2O weight ratios were identical to the H_2SO_4 concentrations in reactions **I** and **IIa**, respectively. A slight lowering trend in the tensile properties was observed with increasing H_2SO_4 concentrations. None of the tensile properties was significantly affected by the sulphuric acid treatments (at the 0.05 significance level), however.

Generally, all the acid- and base-catalysed oxidation reactions lowered the tensile properties of the fibres with increasing reaction times (*Figure 6*). The trends in the reduced tensile properties were different depending upon the reactions. Both acid-catalysed reactions **I** and **IIb** had proper chromic salt to sulphuric acid molar ratios as in equations (1) and (3), respectively. The only distinction between them is the types of chromic salts. The effects of these reactions appeared to be similar at shorter reaction time. At 15 min, however, the tensile properties of the oxidation with CrO_3 were reduced more significantly than those with $K_2Cr_2O_7$. This suggested that chromic acid (**I**) was more effective in oxidizing the UHMWPE fibres than potassium dichromate (**IIb**) when both were assisted with proper molar concentration of sulphuric acid.

The two acid-catalysed reactions with $K_2Cr_2O_7$, i.e. **IIa** and **IIb**, were different only in their sulphuric acid concentrations. The sulphuric acid concentration in reaction **IIa** was 1.5 orders higher than that in reaction **IIb**. The effects of these reactions were similar for the 1 min reactions. At the longer reaction times of 5 and 10 min, however, the tensile properties of the fibres treated by reaction **IIa** deteriorated to a greater extent. Reaction **IIa** had a similar effect on the tensile properties of the fibres as reaction **I**. Although $K_2Cr_2O_7$ was not such an effective oxidant as CrO_3, the effectiveness of $K_2Cr_2O_7$ could be improved by significantly increasing the concentration of sulphuric acid.

The base-catalysed oxidation **III** affected the tensile properties less than the acid-catalysed reaction **IIa** but

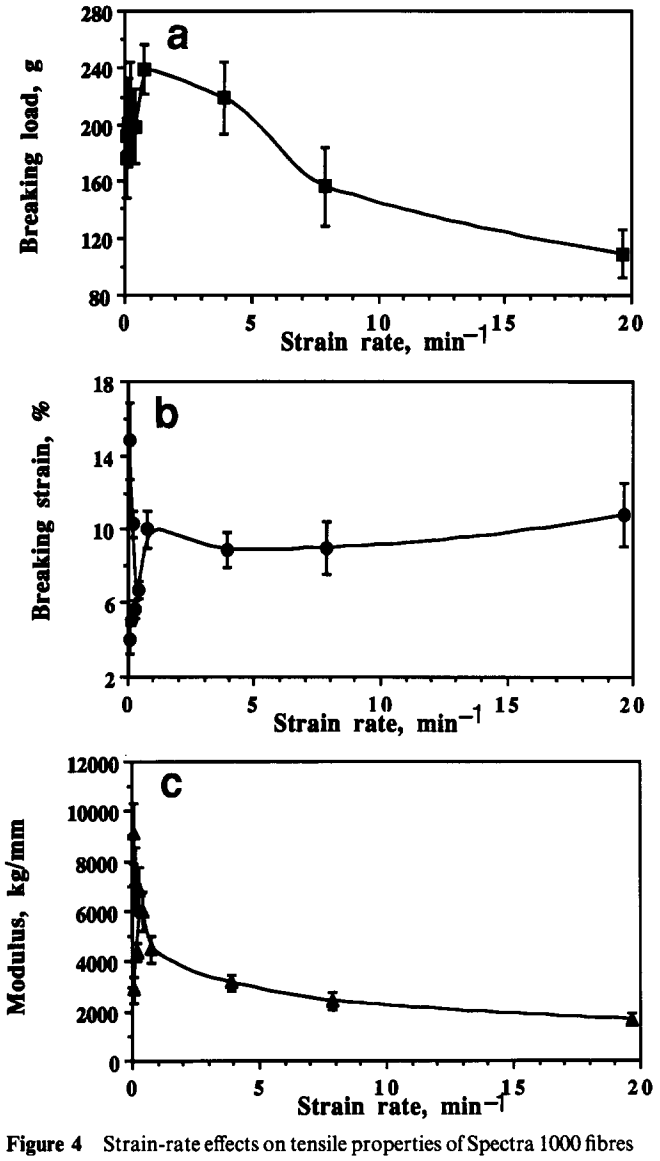

Figure 4 Strain-rate effects on tensile properties of Spectra 1000 fibres

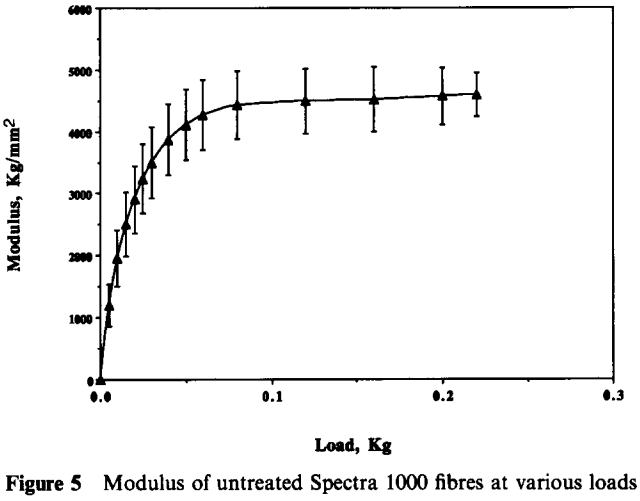

Figure 5 Modulus of untreated Spectra 1000 fibres at various loads

Table 2 Weight changes (%) after oxidative reaction[a]

Time (min)	Acid-catalysed			Base-catalysed
	I	**IIa**	**IIb**	**III**
	CrO_3:H_2SO_4:H_2O	$K_2Cr_2O_7$:H_2SO_4:H_2O		$K_2Cr_2O_7$:NaOH:H_2O
	1:1:1.45	1:20:1.6	1:1.3:1.7	1:0.27:3.3
1	+0.232	+0.347	−0.109	−0.399
5	+0.150	+0.985	−0.456	−0.391
15	+0.139	+0.759	−0.385	−0.351

[a]The three lines below the subheadings show the reaction, the mixture and the weight ratio

Table 3 Tensile properties[a] of sulphuric acid-treated Spectra 1000 fibres

Sulphuric acid:water (wt ratio)	Number of samples	Breaking load (g)	Breaking strain (%)	Breaking energy (g m)	Modulus[b] (kg mm^{-2})
Untreated	14	239.2 (17.4)	10.0 (1.0)	0.320 (0.059)	4485 (524)
1:1.45	15	243.6 (24.2)	10.2 (1.1)	0.299 (0.040)	3831 (676)
3:1	15	228.5 (23.8)	8.6 (0.4)	0.262 (0.041)	4862 (850)
6:1	15	231.2 (27.9)	8.5 (0.5)	0.253 (0.037)	4989 (787)
10:1	15	221.5 (25.2)	9.2 (1.1)	0.252 (0.039)	4269 (871)
12.5:1	15	214.4 (20.4)	9.67 (0.9)	0.255 (0.047)	3768 (786)
27.6:1 (or conc.)	14	214.8 (22.5)	9.3 (0.9)	0.252 (0.049)	4095 (625)

[a]Gauge length = 25.4 mm and crosshead speed = 20 mm min^{-1}
[b]At 100 g load

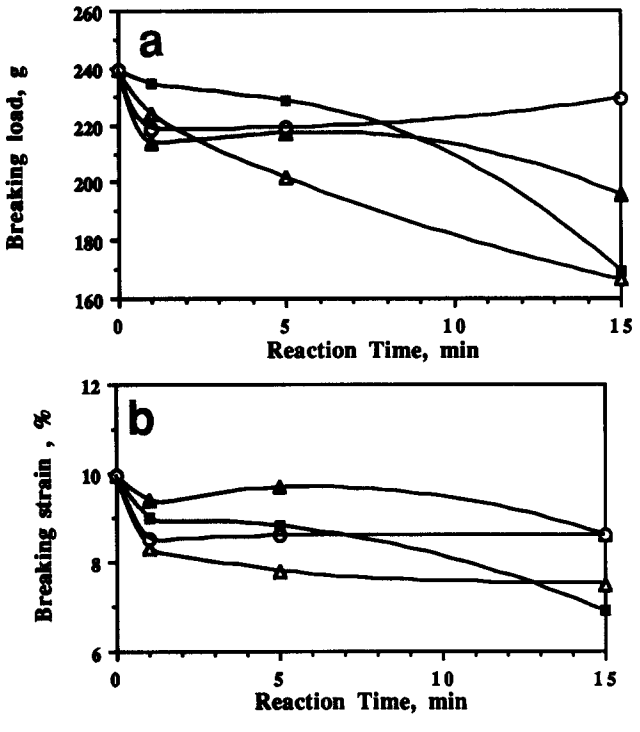

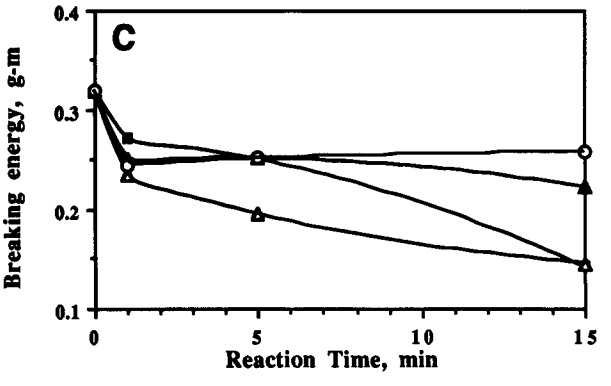

Figure 6 Tensile properties of oxidized Spectra 1000 fibres: reaction I (△), IIa (■), IIb (○), III (▲)

was very similar to the acid-assisted reaction **IIb**. The effects of reaction **III** were also less dependent on the reaction time.

Differential thermal analysis

The d.t.a. thermograph of the untreated UHMWPE fibres (*Figure 7*) showed three distinct melting characteristics including a premelting plateau at 135.8°C, a main melting peak at 154.5°C and a slight shoulder starting at 162°C. The premelting at almost 9°C below the major melting endotherm indicated the existence of smaller and/or less perfect crystallites. The main melting peak is 13°C higher than the 141.4°C equilibrium melting temperature reported for polyethylene[32]. The higher melting temperature of the UHMWPE fibres can be explained by superheating[33] of the large extended-chain crystalline structure. The restriction imposed by intercrystalline tie chains on the crystalline domains can also contribute to the higher melting temperature. The source for the vague shoulder about 7.5°C above the main melting peak is not confirmed at this point.

The thermal behaviour of all oxidized fibres appeared to be similarly affected. The most distinctive changes from the oxidative reactions included the narrower main melting peaks, lowered peak temperatures and the more distinguished post-peak shoulder. The premelting characteristic of the fibres was not altered. The magnitude or temperature of the shoulder peaks also remained unchanged.

The changes observed on the main melting peak further supported the earlier statement that the oxidative attacks occurred on the tie molecules. Oxidative chain scissions at the TTM and entangled molecules reduce the connections in the crystalline network, resulting in lowered melting temperatures and sharper melting peaks. The reduction of tie molecules could lessen intercrystalline stress, leading to increased entropy of fusion. This was found with all reactions (*Table 4*). Using a value of 293 J g^{-1} for the heat of fusion of orthorhombic equilibrium crystals of polyethylene[34], the entropy of fusion increased from the 78.7% of the equilibrium crystals for the untreated UHMWPE fibres to mid-80% for the oxidized fibres.

Surface morphology

The untreated Spectra 1000 fibres had mostly non-cylindrical cross-sectional shapes (*Figure 8a*). The

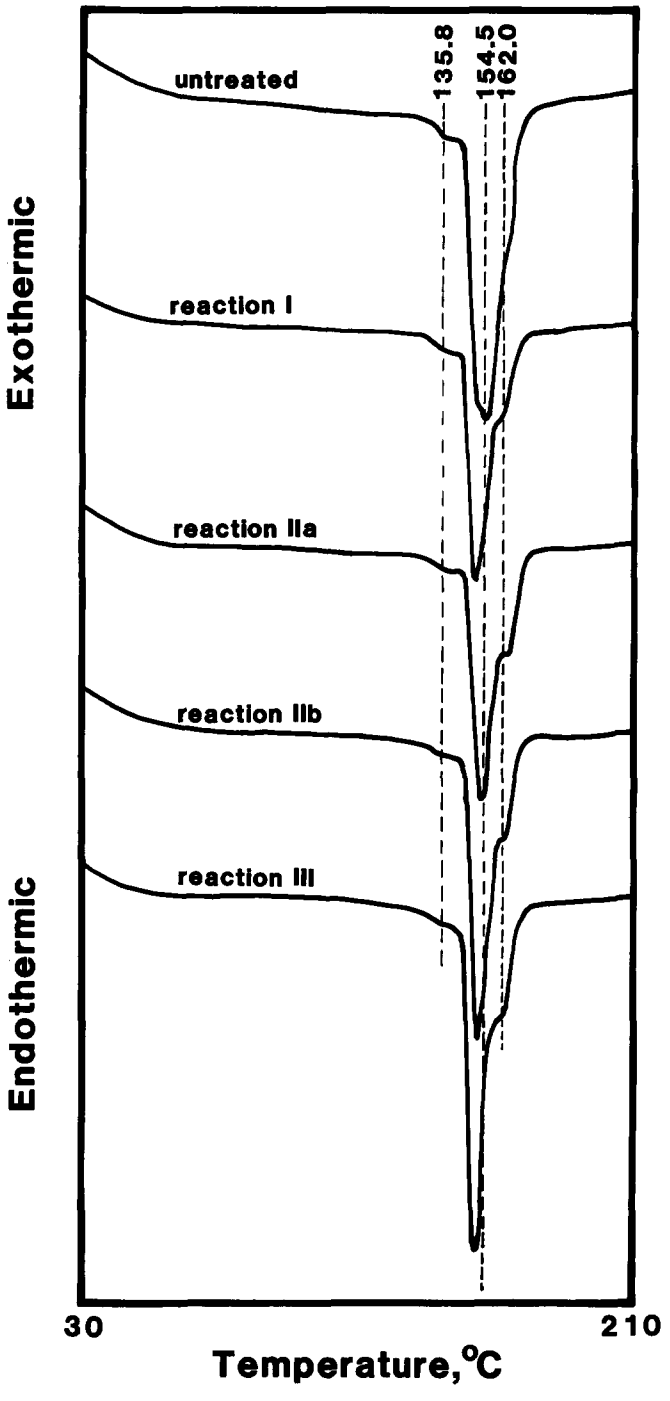

Figure 7 Differential thermal analysis thermograms of Spectra 1000 fibres

fibre surfaces were heavily striated with occasional kink bands (*Figure 8b*). Severe damage to the fibres treated with CrO_3:H_2SO_4:H_2O (1:1:1.45 weight ratio) (*Figure 9a*) and $K_2Cr_2O_7$:H_2SO_4:H_2O (1:20:1.6 weight ratio) (*Figure 9b*) at 68°C for 15 min was observed. The damage was more severe on the former. These fibres easily became melted upon longer exposure under the electron beam in the microscope.

The ends of the fractured untreated fibres appeared fibrillar as reported by others at similar strain rates[31,35]. A stepwise fracture mechanism of breaking through fibrils at weak points and breaking lateral bonds between fibrils

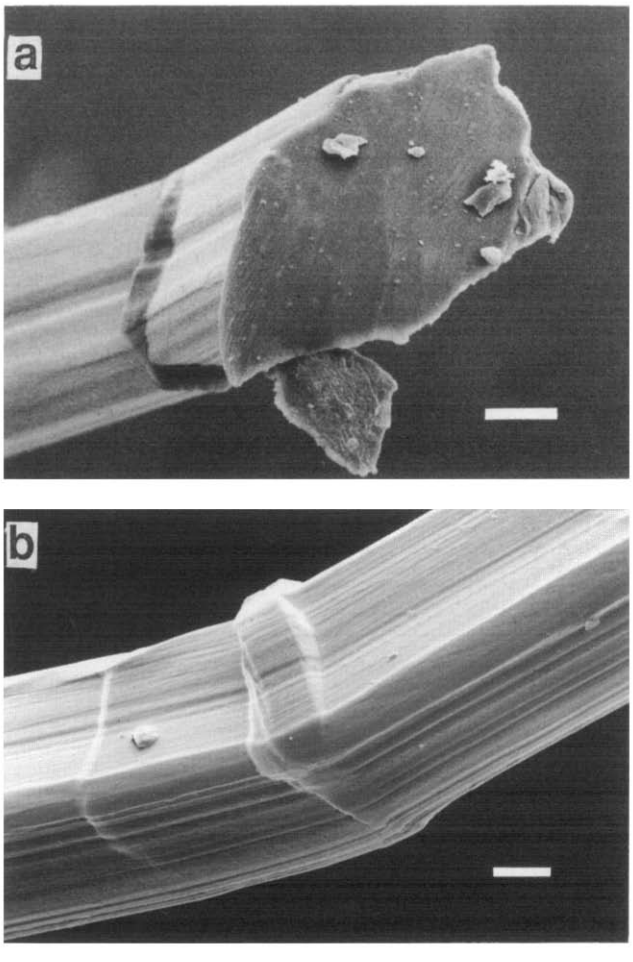

Figure 8 Scanning electron micrographs of untreated Spectra 1000 fibres: (a) bar = 12.6 μm, (b) bar = 8.13 μm

Table 4 Thermal properties[a] of oxidized Spectra 1000 fibres

Reaction		Reaction temperature (°C)	H_f (J g^{-1})	T_m (°C)	Entropy of fusion to equilibrium crystals (%)
None			230.3	154.5	78.7
I	CrO_3:H_2SO_4:H_2O	22	244.0	151.7	83.3
	1:1:1.45	68	254.5	153.3	86.9
IIa	$K_2Cr_2O_7$:H_2SO_4:H_2O	22	243.9	152.7	83.3
	1:20:1.6	68	248.9	151.9	85.0
IIb	$K_2Cr_2O_7$:H_2SO_4:H_2O 1:1.3:1.7	22	247.1	152.5	84.3
III	$K_2Cr_2O_7$:NaOH:H_2O 1:0.27:3.3	22	247.8	151.8	84.6

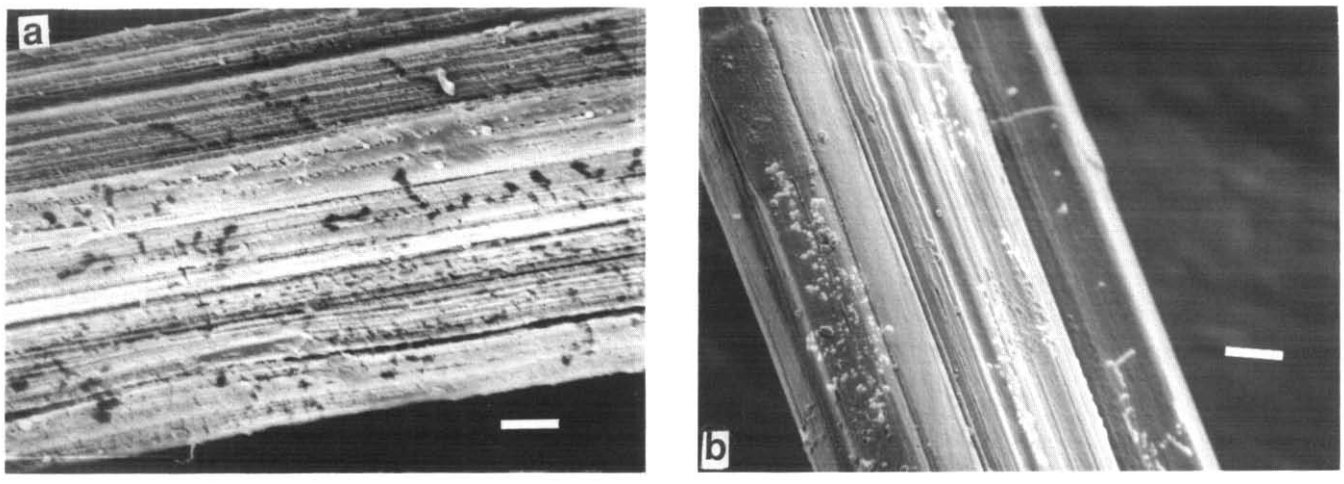

Figure 9 Surfaces of chromic–sulphuric oxidized Spectra 1000 fibres: (a) reaction **I** at 68°C, bar = 5.78 μm, (b) reaction **IIa** at 68°C, bar = 5.75 μm

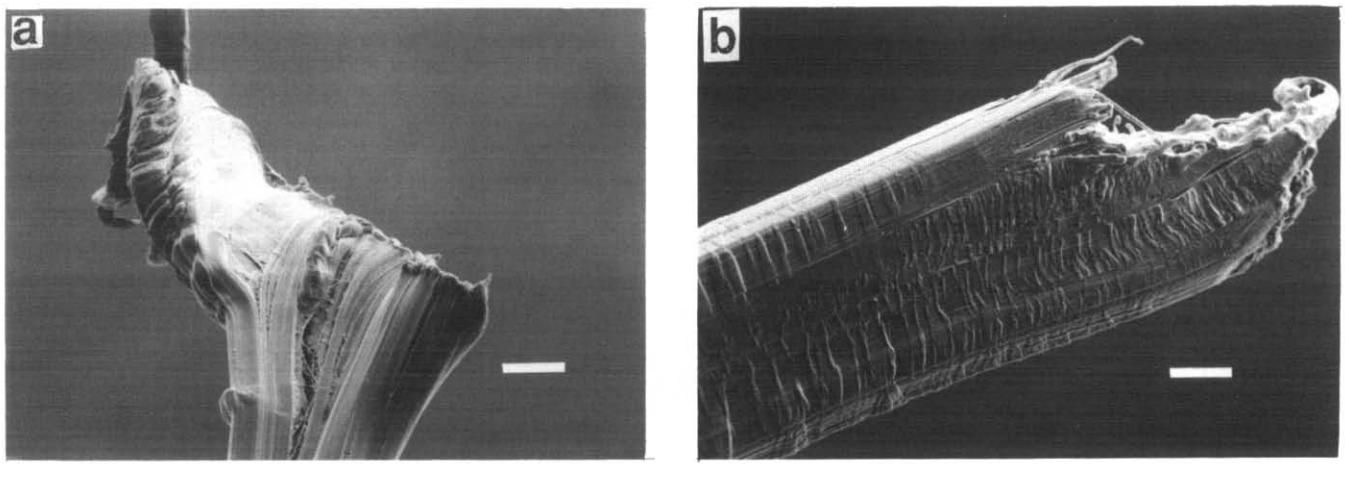

Figure 10 Matching fractured ends of oxidized Spectra 1000 fibres by reaction **I**: (a) bar = 15.5 μm, (b) bar = 9.99 μm

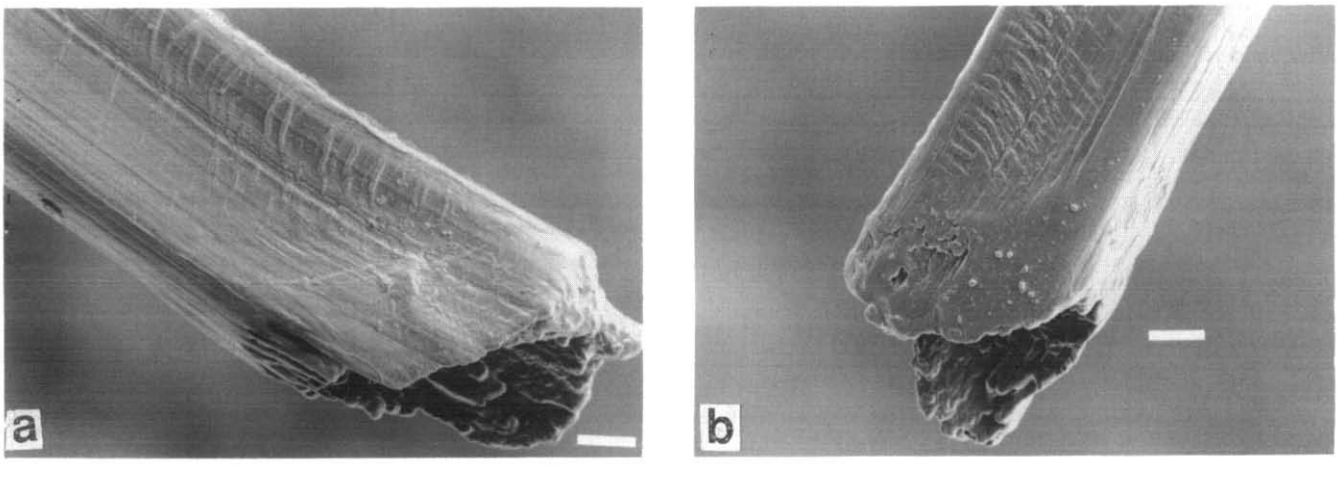

Figure 11 Matching fractured ends of oxidized Spectra 1000 fibres by reaction **IIa**: (a) bar = 7.94 μm, (b) bar = 9.41 μm

was proposed by Peterlin[36] to explain the fibrillated fracture of the untreated fibres. This mechanism was thought to involve cutting (or crack initiation) across a fibril at a defect or weak spot, followed by crack propagation along the broken fibril by breaking interfibrillar bonds until reaching another weak point in the neighbouring fibril.

Matching pairs of broken ends by tensile tests from reactions **I** and **IIa** are shown in *Figures 10* and *11*, respectively. The more abrupt fractured ends indicated brittle failure for the fibres treated by these two reactions. In contrast to the untreated fibre longitudinal separation of the fibrillar structure caused by stress in cutting was also observed at the cut end of fibres from reaction **I**

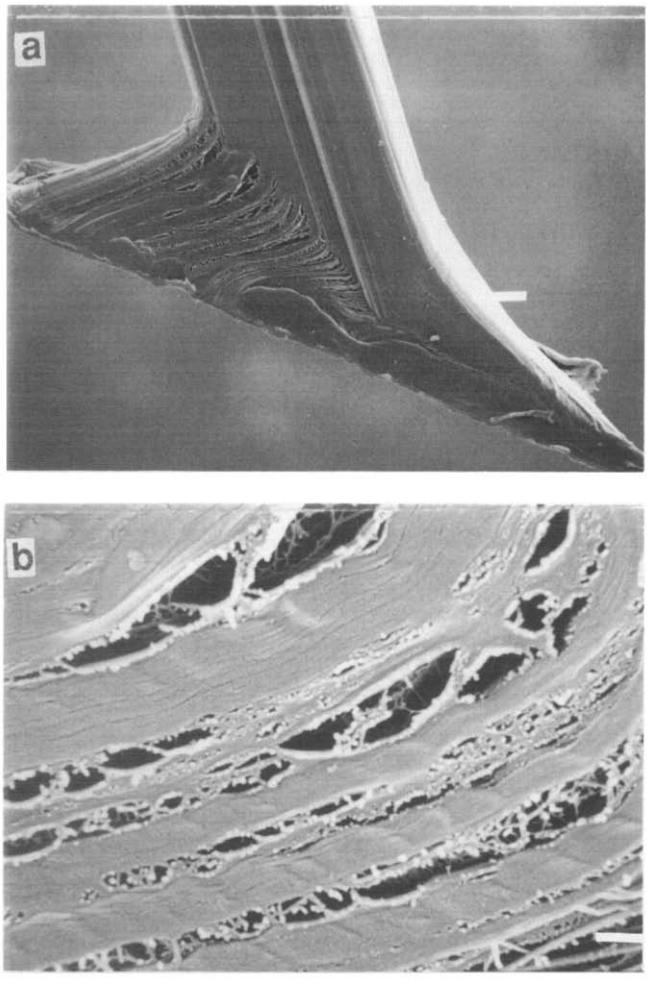

Figure 12 Cut end of oxidized Spectra 1000 fibre by reaction **I**: (a) bar = 10.8 μm, (b) bar = 1.44 μm

(*Figure 12a*). The very distinct fibrillated cracks (*Figure 12b*) indicated weakened lateral bonds among the macrofibrils. Assuming Peterlin's fracture mechanism, the brittle failure of the acid-oxidized fibres also pointed to the occurrence of weak points along the fibril direction in the treated fibres. It was thought that the oxidants attacked the disordered domains that connected the crystal blocks in the microfibrils. The reduced lateral bondings among macrofibrils as well as the weakened disordered domains along the microfibrils indicated more thorough penetration of the acid-catalysed oxidative agents in the fibrillar structures of the UHMWPE fibres by reactions **I** and **IIa**.

The fractured ends of the fibres from the base-catalysed reaction **III**, on the other hand, remained fibrillated (*Figure 13*) as observed on the untreated fibres. The tensile properties of fibres oxidized by the base-catalysed reaction was less severe and less time-dependent. Considering the stepwise mechanism of breaking through fibrils at weak points and interfibril lateral bonds, the fibrillated fracture by the base-catalysed reaction suggested that the penetration and oxidative attacks were predominantly in the interfibrillar regions of the fibres.

On all oxidized fibres, some elevated surface features were observed on the fractured fibres perpendicular to the fibre axis (*Figures 10, 11* and *13*). On the less oxidized fibres such as those from reaction **III** and reaction **I** with shorter reaction time, wide bands (*Figure 13b*) similar to the kink bands on the untreated fibres (*Figure 8b*) were found. These band widths ranged from a few micrometres to about 15 μm. On the highly oxidized fibres (reaction **I** for 15 min), much finer and laterally isolated textures were observed. The widths of these textures were at least one magnitude lower than the kink band. The distinctive differences between these two groups of fibres indicated the sources of these surface features were reaction-related. The fine textures perpendicular to the fibre axis may very well be related to the more thorough penetration and oxidative attacks at the disordered regions along the microfibrils as proposed for reactions **I** and **IIb**.

SUMMARY

The single-fibre tensile properties of the untreated UHMWPE fibres were found to be dependent on both gauge length and crosshead speed within the 0 to 20 min^{-1} strain-rate range studied. The strain-rate dependence of the fibres at low strain rates up to 1 min^{-1} was especially distinctive depending upon the strain-rate variable. The optimal breaking load (239 g) was obtained at a 25.4 mm gauge length whereas the optimal breaking strain (4.0%) and modulus (9101 kg mm^{-2}) were found at a much longer 254 mm gauge length, all at a 20 mm min^{-1} crosshead speed. The tensile properties of all fibres were compared using a 25.4 mm gauge length and a 20 mm min^{-1} crosshead speed, or a 0.787 min^{-1} strain rate.

The acid-assisted reactions with CrO_3 (**I**) and with

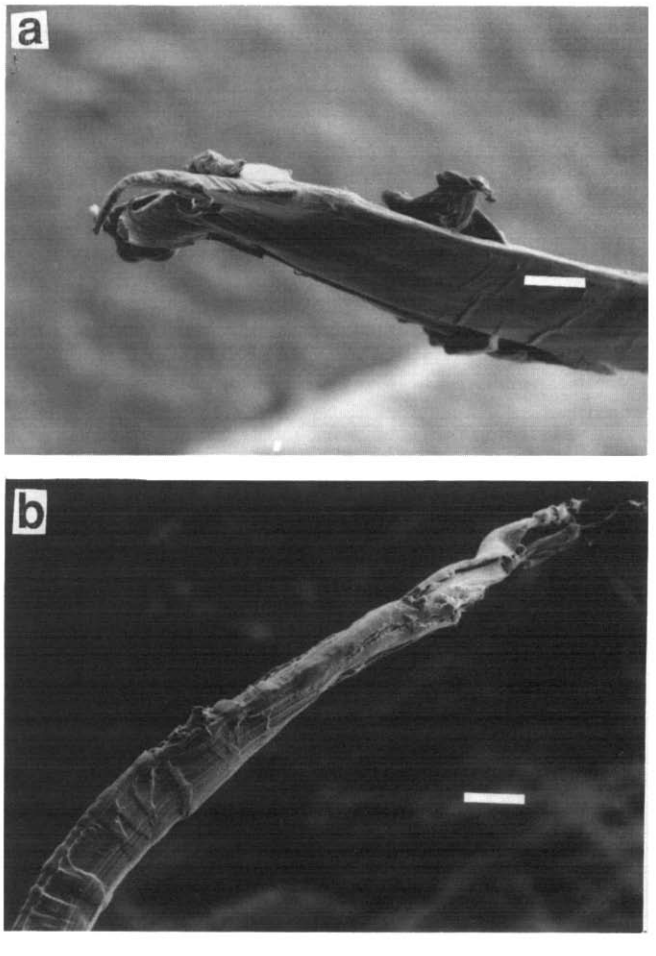

Figure 13 Matching fractured ends of oxidized Spectra 1000 fibre by reaction **III**: (a) bar = 18.3 μm, (b) bar = 26.3 μm

$K_2Cr_2O_7$ at a higher sulphuric acid concentration (**IIa**) caused the tensile properties of fibres to deteriorate to a greater extent and were highly reaction-time-dependent as compared to the less time-dependent effects of reactions **IIb** and **III**. Considering the stepwise mechanism of breaking through fibrils at weak points and interfibril lateral bonds, the fibrillated fractures and tensile properties that resulted from reactions **IIb** and **III** could be explained by the predominantly interfibrillar penetration and oxidative attacks. More thorough penetration of oxidants and weakened disordered domains along the microfibrils were believed to cause the brittle fractures of fibres treated with reactions **I** and **IIa**.

The untreated UHMWPE fibres showed a premelting region at around 135.8°C, a main melting peak at 154.5°C and a slight shoulder starting at 162°C. This higher main melting temperature than that of the equilibrium crystals was due to superheating. The effects of all oxidative reactions on the melting behaviour were similar, i.e. narrowed main melting peaks, lowered peak temperatures and increased heat of fusion. The observed effects on the main melting peak could be explained by the oxidative chain scissions of the taut tie molecules. The reduced connection in the crystallite network allowed greater movement of crystallites, thus reducing superheating. The reduction of intercrystalline stress also contributed to the increased entropy of fusion.

REFERENCES

1 Gerenser, L. J., Elman, J. F., Mason, M. G. and Pochan, J. M. *Polymer* 1985, **26**, 1162
2 Gerenser, L. J. *J. Adhes. Sci. Tech.* 1987, **1** (4), 303
3 Briggs, D., Zichy, V. J. I., Brewis, D. M., Comyn, J., Dahm, R. H., Gree, M. A. and Konieczko, M. B. *Surf. Interface Anal.* 1980, **2** (3), 107
4 Holmes-Farley, S. R., Bain, C. D. and Whitesides, G. M. *Langmuir* 1988, **4**, 921
5 Holmes-Farley, S. R., Reamey, R. H., McCarthy, T. J., Deutch, J. and Whitesides, G. M. *Langmuir* 1985, **1**, 725
6 Briggs, D., Brewis, D. M. and Konieczko, M. B. *J. Mater. Sci.* 1976, 1270
7 Ward, I. M. and Ladizesky, N. H. in 'Composite Interfaces' (Eds H. Ishida and J. L. Koenig), North-Holland, New York, 1986
8 Nardin, M. and Ward, I. M. *Mater. Sci. Technol.* 1987, **3**, 814
9 Ishida, I. *Proc. ACS Div. Polym. Mater. Sci. Eng.* 1988, **59**, 919
10 Southern, J. H. and Porter, R. S. *J. Appl. Polym. Sci.* 1970, **14**, 2305
11 Pennings, A. J., Zwijnenburg, A. and Lageveen, R. *Kolloid Z.Z. Polym.* 1973, **251**, 500
12 Capaccio, G. and Ward, I. M. *Polymer* 1974, **15**, 233
13 Smith, P., Lemstra, P. J., Kalb, B. and Pennings, A. J. *Polym. Bull.* 1979, **1**, 733
14 Sawatari, C. and Matsuo, M. *Colloid. Polym. Sci.* 1985, **263**, 783
15 Smook, J., Flinterman, M. and Pennings, A. J. *Polym. Bull.* 1981, **5**, 317
16 Barham, P. J. and Arridge, R. B. C. *J. Polym. Sci., Polym. Phys. Edn* 1977, **15**, 1177
17 Klein, P. G., Ladizesky, N. H. and Ward, I. M. *J. Polym. Sci., Polym. Phys. Edn* 1986, **24**, 1093
18 Mead, W. T., Cesper, C. R. and Porter, R. S. *J. Polym. Sci., Polym. Phys. Edn* 1979, **17**, 859
19 Peterlin, A. *Polym. Eng. Sci.* 1969, **9**, 172
20 Lemstra, P. J., van Aerle, N. A. J. M. and Bastlaansen, C. W. M. *Polym. J.* 1987, **19**, 85
21 Smith, P., Chanzy, H. D. and Rotzinger, B. P. *Polym. Commun.* 1985, **26**, 258
22 Zachariades, A. E. and Kanamoto, T. 'High Modulus Polymers with Stiff and Flexible Chains' (Ed. A. E. Zachariades and R. S. Porter), Marcel Dekker, New York, 1987
23 Dijkstra, D. J. and Pennings, A. J. *Polym. Bull.* 1988, **19**, 73
24 Smook, A. J. and Pennings, A. J. *Colloid Polym. Sci.* 1984, **262**, 712
25 Zwijnenburg, A., van Hutten, P. F., Pennings, A. J. and Chanzy, H. D. *Colloid Polym. Sci.* 1978, **256**, 729
26 Peterlin, A. *Polym. Eng. Sci.* 1969, **9**, 172
27 Peterlin, A. 'Ultra-high Modulus Polymers' (Eds A. Cifferi and I. M. Ward), Applied Science, London, 1979
28 Peterlin, A. *J. Macromol. Sci. Phys. (B)* 1973, **8** (1–2), 83
29 Dijkstra, D. J. and Pennings, A. J. *Polym. Bull.* 1987, **17**, 507
30 Kato, K. *J. Appl. Polym. Sci.* 1976, **20**, 2451
31 Schwartz, P., Netravali, A. and Sembach, S. *Textile Res. J.* 1986, **56** (8), 502
32 Hellmuth, E. and Wunderlich, B. *J. Appl. Phys.* 1965, **36**, 3039
33 Wunderlich, B. 'Macromolecular Physics', Vol. 3, Academic Press, London, 1980, Ch. 8
34 Wunderlich, B. and Czornyj, G. *Macromolecules* 1977, **10**, 906
35 Smook, A. J., Hamersma, W. and Pennings, A. J. *J. Mater. Sci.* 1984, **19**, 1359
36 Peterlin, A. *J. Macromol. Sci., Phys. (B)* 1981, **19**, 409